Published in final edited form as:
Cancer Res. 2011 January 1; 71(1): 216–224. doi:10.1158/0008-5472.CAN-10-1725.

Biological Activity of 4-Substituted Methoxybenzoyl-Aryl-Thiazole (SMART): An Active Microtubule Inhibitor

Chien-Ming Li[a,b,#], **Zhao Wang**[c,#], **Yan Lu**[c], **Sunjoo Ahn**[a,b], **Ramesh Narayanan**[b], **Jeffrey D. Kearbey**[b], **Deanna N. Parke**[b], **Wei Li**[c,*], **Duane D. Miller**[b,c], and **James T. Dalton**[a,b,*]

[a] Division of Pharmaceutics, College of Pharmacy, The Ohio State University, Columbus, OH, 43210

[b] Preclinical Research and Development, GTx Inc., Memphis, TN 38163

[c] Department of Pharmaceutical Sciences, University of Tennessee Health Science Center, Memphis, TN 38163

Abstract

Formation of microtubules is a dynamic process that involves polymerization and depolymerization of αβ-tubulin heterodimers. Drugs that enhance or inhibit tubulin polymerization can destroy this dynamic process, arresting cells in the G_2/M phase of the cell cycle. Although drugs that target tubulin generally demonstrate cytotoxic potency in the sub-nanomolar range, resistance due to drug efflux is a common phenomenon among the antitubulin agents. We recently reported a class of 4-Substituted Methoxybenzoyl-Aryl-Thiazoles (SMART) that exhibited great *in vitro* potency and broad spectrum cellular cytotoxicity. Evaluation of the *in vitro* and *in vivo* anti-cancer activities of three SMART compounds, SMART-H (H), SMART-F (F) and SMART-OH (OH) with varying substituents at the 4-position of aryl ring, demonstrated that they bind potently to the colchicine binding site in tubulin, inhibit tubulin polymerization, arrest cancer cells in G_2/M phase of the cell cycle, and induce their apoptosis.

The SMART compounds also equi-potently inhibit the growth of parental and MDR-over-expressing cells *in vitro*, indicating that they can overcome multidrug resistance. *In vivo* anti-tumor efficacy studies in human prostate (PC-3) and melanoma (A375) cancer xenograft models demonstrated that SMART-H and SMART-F treatments resulted in %T/C values ranging from 4–30%. In addition, *in vivo* SMART-H treatment for 21 days at the higher dose (15 mg/kg) failed to produce any apparent neurotoxicity. These studies provide the first *in vivo* evidence and proof-of-concept that SMART compounds are similarly efficacious to currently FDA approved antitubulin drugs for cancer treatment, but they can circumvent P-glycoprotein-mediated drug resistance.

Keywords

tubulin; P-glycoprotein; pharmacokinetics; xenograft

Introduction

Microtubules, composed of αβ-tubulin heterodimers, play an important role in cell mitosis, motility and organelle distribution (1). Formation of microtubules from tubulin is a dynamic

[*]To whom correspondence should be addressed. James T. Dalton, Telephone: (901)507-8604. Fax: (901)523-9772. jdalton@gtxinc.com, Wei Li, Telephone: (901)448-7532. Fax: (901)448-6828. wli@uthsc.edu.
[#]These authors contributed equally.

process that involves polymerization and depolymerization and is crucial for mitosis (2). Interference with tubulin-microtubule dynamics is one of the most attractive and successful molecular strategies to treat cancer (3,4). Paclitaxel, docetaxel, ixabepilone and three vinca alkaloids (vinblastine, vincristine, and vinorelbine), all FDA approved drugs, effectively inhibit tubulin action and successfully treat cancer (5).

The taxanes and epothilones are semi-synthetic natural products that stabilize microtubules and cause apoptosis (5). Paclitaxel and ixabepilone occupy overlapping binding sites on the surface of β-tubulin (6) and demonstrate nanomolar cytotoxicity in a variety of cancer cell lines. Unlike paclitaxel and docetaxel, ixabepilone demonstrates reduced susceptibility to drug resistance mechanisms that limit the effectiveness of taxanes, anthracyclines and a host of other anticancer agents (7). The over-expression of ATP binding cassette (ABC) proteins, most notably P-glycoprotein (P-gp), in many cancer cells and tumors results in innate or acquired resistance to chemotherapy (8). The ability of ixabepilone to circumvent these multidrug resistance (MDR) mechanisms has provided a unique chemotherapeutic approach for patients with anthracyclines or taxanes resistant tumors. An orally bioavailable sulfonamide (ABT-751) that inhibits tubulin polymerization and maintains activity in cells expressing P-glycoprotein is currently being evaluated in phase I trials (9,10), but is not yet available for routine clinical use. Despite the widespread use of the vinca alkaloids for the treatment of cancer and their susceptibility to these same MDR mechanisms, an anticancer agent that destabilizes microtubules and effectively circumvents P-gp-mediated drug resistance is not yet approved for clinical use.

We recently reported the synthesis and *in vitro* anticancer characterization of a novel series of 4-Substituted Methoxybenzoyl-Aryl-Thiazoles (SMART) (11). SMART compounds were synthesized in a simple four-step procedure, providing a method for rapid and high yield synthesis of a variety of analogs. Compounds with an un-substituted aryl ring (SMART-H) or bearing a 4-fluoro substituent (SMART-F) were the most active, with IC_{50} values ranging from 6 to 55 nM. The earlier report further revealed that the presence of 3, 4, 5-trimethoxyphenyl ring is essential for the inhibition of tubulin function.

In the present study, we synthesized and characterized an additional 4-hydroxy SMART compound (SMART-OH) to improve the solubility of the parent SMART-H. We examined the binding of SMART-H to tubulin, demonstrated that the compounds inhibit tubulin polymerization via binding to the colchicine binding site on tubulin, show that these compounds circumvent P-gp-mediated MDR, and demonstrate promising *in vivo* antitumor activity in mice bearing human prostate cancer (PC-3) and melanoma (A375) tumors. The discovery of these SMART drugs may provide a novel pharmacologic alternative to the MDR exhibited by several cancers upon prolonged exposure to taxane, anthracycline and the vinca alkaloids.

Materials and Methods

In vitro microtubule polymerization assay

Bovine brain tubulin (0.4 mg) (Cytoskeleton, Denver, CO) was mixed with 10 μM of the test compound or vehicle (DMSO) and incubated in 100 μl of buffer (80 mM PIPES, 2.0 mM $MgCl_2$, 0.5 mM EGTA, pH 6.9 and 1 mM GTP). The absorbance at 340 nm wavelength was monitored every min for 15 min (SYNERGY 4 Microplate Reader, Bio-Tek Instruments, Winooski, VT). The spectrophotometer was maintained at 37 °C for tubulin polymerization.

Cell culture and cytotoxicity assay of prostate carcinoma and melanoma cell lines

All prostate cancer cell lines (LNCaP, PC-3, and DU145, PPC-1) and melanoma cell lines (A375 and WM-164) were obtained from ATCC (American Type Culture Collection,

Manassas, VA, USA). Human ovarian cell line OVCAR-8 and its resistant cell line that over-expresses P-gp, NCI/ADR-RES, were used as MDR models. Both ovarian cell lines were obtained from National Cancer Institutes (NCI). All cell lines were tested and authenticated by either ATCC or NCI. All cell lines obtained from ATCC or NCI were immediately expanded and frozen down such that all cell lines could be restarted every 2~3 months from a frozen vial of the same batch of cells. Cell culture supplies were purchased from Cellgro Mediatech (Herndon, VA, USA). All cell lines were used to test the antiproliferative activity of SMART compounds by sulforhodamine B (SRB) assay as previous described (11). All prostate and ovarian cancer cell lines were maintained in RPMI 1640 media with 2mM L-glutamine and 10% fetal bovine serum (FBS), while melanoma cancer cell lines were maintained in DMEM media with 2mM L-glutamine and 5% FBS.

Cell cycle analysis

Flow cytometry was performed to study the effects of the SMART compounds on cell cycle distribution. PC-3 and A375 cells were treated in growth media with the indicated concentrations of SMART-H, -F, and -OH for 24 h. Cellular DNA was stained with 100 μg/mL propidium iodide and 100 μg/mL RNase A in PBS and flow cytometry was performed to determine the cell cycle distribution of the cells.

Apoptosis detection by ELISA

Quantification of the enrichment of mono-and oligo-nucleosomes in the cytoplasm was used to determine the ability of the SMART compounds to induce apoptosis (cell death detection ELISA PLUS, Roche, Germany) following the manufacturer's instructions.

Pharmacokinetic study

Male ICR mice (n = 3 or 4 per group) 6 to 8 weeks of age were purchased from Harlan Inc., and used to examine the pharmacokinetics (PK) of the SMART compounds. SMART-F, and –OH (15 mg/kg) were dissolved in PEG300/DMSO (1/4) and administered by a single i.v. injection into the tail vein. Blood samples were collected at 2, 5, 15, and 30 min, 1, 2, 4, 8, 16, and 24 hr after administration.

Male Sprague-Dawley rats (n = 4; 254 ± 4 g) were purchased from Harlan Inc. (Indianapolis, IN). SMART-F was administered intravenously into the jugular venous catheters at 2.5 mg/kg (in DMSO/PEG300, 1/4). Blood samples (250 μL) were collected at 10, 20, 30 min, and 1, 2, 4, 8, 12, 24, 48hr.

A protein precipitation method was used for sample preparation. An aliquot (200 μL) of acetonitrile (ACN) was added to 100 μL of plasma and then was thoroughly vortexed for 15 s. After centrifugation, the supernatant was analyzed by liquid chromatography tandem mass spectrometry (LC-MS/MS). The PK parameters were determined using Non compartmental analysis (WinNonlin, Pharsight Corporation, Mountain View, CA)

PC-3 and A375 tumor xenograft studies

PC-3 and A375 cells (5×10^7 per ml) were prepared in phenol red-free growth media containing 10% FBS, and mixed with Matrigel (BD Biosciences, San Jose, CA) at 1:1 ratio. Tumors were established by injecting 100 μL of the mixture (2.5×10^6 cells per animal) subcutaneously (s.c.) into the flank of 6–8-week-old male athymic nude mice. Length and width of tumors were measured and the tumor volume (mm^3) was calculated by the formula, $\pi/6 \times L \times W^2$, where length (L) and width (W) were determined in mm. When the tumor volumes reached 150 mm^3, the animals bearing PC-3 tumors were treated intraperitoneally with vehicle [Captex200/Tween80 (1/4)], SMART-H (5 and 15 mg/kg), SMART-F (5 and 15 mg/kg) and SMART-OH (50 mg/kg) intraperitorally for 21 days. Vinblastine (0.5 mg/kg)

was used as the positive control and dosed q2d with vehicle [DMSO/PEG300 (1/9)]. On the other hand, A375 tumor bearing mice were treated for 34 days with vehicle [Captex200/Tween80 (1/4)], SMART-H (20 mg/kg) or SMART-F (15 mg/kg). Doses were selected based on acute toxicity studies of SMART-H and SMART-F in ICR mice (n = 2/group) showing that doses up to 30 mg/kg and 15 mg/kg, respectively, did not cause greater than 10% loss of body weight after 4 consecutive days of intraperitoneal dosing.

In vivo antitumor activity

Evidence of drug effect is described by the following parameters: %T/C = [Δ tumor volume of treated group]/[Δ tumor volume of control group] × 100%. By National Cancer Institute criteria, agents which confer %T/C < 40% are considered to be minimally active, and %T/C < 10% are considered to be highly active (12).

Rotarod test

ICR mice received training three times a day for two days to enable them to stay on the rotating rod for >120 seconds at 12 rpm. Mice were then randomized by the length of time that they could stay on the rotating rod and divided into 7–8 mice per group. SMART-H at a dose of 5 or 15 mg/kg in Captex200/Tween80 (1/4) was administered by intraperitoneal injection. Vinblastine at a dose of 0.5 mg/kg/day was used as a positive control under the same conditions. The rotarod test was performed twice a week. Treatment was stopped on day 31, and post observation was examined on weeks 1, 2, and 4 after termination of the treatment. The rod speed was increased from 5 rpm to 40 rpm over a period of 5 min. Performance was measured as the length of time that a mouse could stay on the rotating rod.

In vivo drug resistance studies

At the end of the PC-3 xenograft studies, solid tumors from control and SMART-H treated (15 mg/kg) groups were removed and digested with 0.1% collagenase (Type I) and 50 mg/ml DNAse (Worthington Biochemical Corp., Freehold, NJ). Dispersed cells were plated in RPMI medium + 10% FBS and incubated at 37°C and 5% CO_2 for 24 hr to allow attachment. The anti-proliferative effects of SMART-H were compared to determine whether tumor cells remaining in PC-3 xenografts retained sensitivity to drug. The PC-3 cells obtained from ATCC were used as *in vitro* control. Statistical analyses were performed using simple Students t-Test.

Results

Based on structure-activity relationship studies, three SMART compounds (Fig. 1A) were selected for biological characterization. While SMART-H and SMART-F are highly potent molecules with low nanomolar cytotoxic properties, SMART-OH, which was rationally designed as a potential metabolite with improved solubility, had the least potent anti-proliferative effects (Table 1).

SMARTs inhibit microtubule polymerization by binding to the colchicine binding site on tubulin

Bovine brain tubulin (>97% pure) was incubated with the individual SMART compounds (10 μM) to test their effect on tubulin polymerization (Fig. 1B). While SMART-H and SMART-F inhibited tubulin polymerization by 90%, SMART-OH inhibited the polymerization by only 55%. Previous studies demonstrated a concentration-dependent inhibition of tubulin polymerization by SMART-H. In addition, under the same experimental conditions, the IC_{50} for SMART-H (4.23 μM) is similar to that of colchicine

(4.91 μM). These data suggest that SMART compounds exhibit strong antitubulin polymerization activity that corresponds well with their cytotoxicity (Table 1).

The ability of the SMART compounds to compete for known binding sites on tubulin was determined using a novel MS competitive binding assay, which was developed in our laboratory (C. M. Li et al, in press). Three tubulin ligands, corresponding to the three binding sites on tubulin, colchicine, vinblastine, and paclitaxel were used for these competitive binding studies. We found that, SMART-H specifically competed with colchicine binding to tubulin, but it did not compete with either vinblastine or paclitaxel binding to tubulin.

SMART compounds inhibit the growth of multidrug-resistant cancer cell lines

The ability of SMART compounds to inhibit the growth of cancer cell lines was evaluated using the SRB assay. As shown in Table 1, the SMART compounds inhibited the growth of several human cancer cell lines, including four prostate cancer cell lines, and two melanoma cell lines, with IC_{50} values in the low nanomolar range. Out of the three SMART compounds, SMART-OH was the least potent (IC_{50} 76~116 nM). SMART-F exhibited the best anti-proliferative effect with IC_{50} values between 6 and 43 nM in prostate cancer and melanoma cell lines. In addition, the effect of SMART compounds in the OVCAR-8 and NCI/ADR-RES cell lines was also evaluated (Table 1). SMART compounds were equally potent against MDR cell (NCI/ADR-RES) and the parent cell line (OVCAR-8). Paclitaxel, vinblastine, and colchicine exhibited relative resistance values of 1333, 149, and 65 times, respectively. These data indicate that the SMART compounds circumvent P-gp-mediated drug resistance.

SMART compounds arrest PC-3 (Prostate) and A375 (Melanoma) cells in G_2/M phase of cell cycle and induce cell apoptosis

PC-3 and A375 cells were exposed to 10, 50, 200, and 1000 nM of SMART compounds for 24 h. Treatment of both cell lines with SMART compounds resulted in concentration-dependent accumulation of both PC-3 and A375 cells in the G_2/M phase with concomitant decreases in the percentage of cells in G_0/G_1 phase (Fig. 2A and 2B). The proportion of cells in G_2/M phase significantly increased when treated with 50 to 200 nM of SMART-H, –F, and -OH.

Apoptosis was then examined by measuring the level of cytoplasmic DNA-histone complexes in PC-3 and A375 cells after 24 h treatment. Increasing concentration of the SMART compounds increased the level of cytoplasmic DNA-histone complexes in PC-3 and A375 cells (Fig. 2C and 2D). The effect was more pronounced in A375 cells than PC-3 cells, but apoptosis was evident in both cell types. SMART-H and SMART-F induced moderate apoptosis at a concentration of 50 nM, while SMART-OH induced apoptosis only at concentrations ≥ 200 nM.

In vivo PK profile of SMART compounds

A single bolus dose of SMART-F and -OH (15 mg/kg) was administered by tail vein injection to ICR mice to characterize their pharmacokinetics (Fig. 3A). SMART-H and -F exhibited similar PK properties, but SMART-OH exhibited slightly greater AUC than SMART-H and SMART-F, indicative of a lower clearance for SMART-OH (Table 2). SMART-OH also had 2–3 times higher V_{ss} than that of SMART-H and –F. The clearance values for all three SMARTs were ≥ 90 ml/min/kg (the hepatic blood flow rate in mice (13)), suggesting that in addition to hepatic removal, other degradation routes may be involved in the elimination of SMARTs.

The pharmacokinetics of SMART-F (2.5 mg/kg) was also examined in rats (Fig. 3B). Interestingly, low clearance values and hepatic extraction rates were obtained by SMART-F and -H (Table 2), suggesting that SMART compounds exhibit species differences in clearance. In rats, SMART-H and -F exhibited favorable pharmacokinetic properties, which are low clearance, moderate volume of distribution, long half-life, and high exposure (AUC) (Table 2).

SMART compounds inhibit prostate and melanoma xenografts growth without neurotoxicity

PC-3 prostate cancer and A375 melanoma tumor xenografts in mice were allowed to reach a volume of 150 mm^3 and then tumor-bearing mice were treated with the SMART compounds. As shown in Fig. 4A, tumor volumes in the control group increased to 680 ± 198 mm^3 over the 21 day duration of the study. Tumor volumes in the SMART-H-treated group increased to 370 ± 103 mm^3 (5 mg/kg treatment) and 176 ± 112 mm^3 (15 mg/kg treatment) by day 21, indicating effective anti-tumor activity for this compound. Tumors in the SMART-F-treated animals increased to 269 ± 177 mm^3 (5 mg/kg treatment) and 292 ± 103 mm^3 (15 mg/kg treatment), while animals in the SMART-OH (50 mg/kg) treated group had tumors of 331 ± 130 mm^3 at day 21. This reduction in tumor volume reversed upon withdrawal of SMART compounds (data not shown). Table 3 summarized the *in vivo* efficacy (%T/C) of SMART compounds. SMART-H tumor elicited %T/C = 29% and 4% at 5 and 15 mg/kg treatment, respectively, whereas, SMART-F elicited %T/C of 21% and 24% at 5 and 15 mg/kg treatment, respectively. The high dose of SMART-OH (50 mg/kg) exhibited the %T/C of 34%. Vinblastine, the positive control, showed %T/C of 29% at day 22 in PC-3 xenografts (Fig. 4B). Body weight measurements, to monitor toxicity, indicated that only 1 of 8 mice treated with SMART-H (15 mg/kg), and 2 out of 7 mice treated with SMART-F (15 mg/kg) lost more than 15 % body weight. In addition to the antitumor effects of the SMART compounds on PC-3 prostate tumors, SMART-H (20 mg/kg) and SMART-F (15 mg/kg) demonstrated a significant reduction of A375 tumors. As shown in Fig. 4C, the tumor volumes of control group increased to 2183 ± 279 mm^3, whereas the volumes in SMART-H and SMART-F treatment groups increased to 775 ± 107 mm^3 and 722 ± 135 mm^3, respectively. SMART-H and SMART-F treatment resulted in %T/C indices of 28% and 29 %, respectively.

Rotarod tests were performed to examine the possible *in vivo* neurotoxic effects of SMART-H. Based on the result of *in vivo* efficacy experiments, 5 or 15 mg/kg [i.p. administration, Captex200/Tween80 (1/4)] of SMART-H was chosen to study the effect on motor coordination. A 0.5 mg/kg treatment with vinblastine was used as the positive control under the same conditions. As shown in Fig. 4D, vinblastine gradually reduced the time (in seconds) that the mice could stay on the rotating rod, and attained significance by days 27 and 31 ($p < 0.05$) compared to the vehicle group. However, no significant difference was observed in the SMART-H treatment groups, suggesting that SMART-H did not cause neurotoxicity in ICR mice at doses that are associated with antitumor effects.

SMART-H did not develop drug-resistance in PC-3 tumor bearing mice

We excised the PC-3 tumors from nude mice after 21 days of treatment with vehicle (n = 3) or 15 mg/kg SMART-H (n = 3). Solid tumors were digested and dispersed into cells as described in the methods section. PC-3 cell line from ATCC (American Type Culture Collection, Manassas, VA, USA) was used as a control. IC_{50} values were 29.1 ± 1.1, 29.1 ± 0.8, and 30.4 ± 0.5 nM in PC-3 cells from ATCC, and dissociated cells from vehicle and SMART-H treated tumors, respectively. These data demonstrate that SMART-H did not induce drug-resistance in PC-3 tumors after 21 days of continuous SMART-H treatment.

Discussion

The general molecular mechanism of action of antitubulin agents is to bind to microtubules, arrest cells in G_2/M phase, and cause cell apoptosis. In this study, we examined the ability of three novel SMART compounds to bind tubulin, inhibit its polymerization and induce apoptosis in two tumor cell types. The SMART compounds bound to the colchicine binding site in tubulin, disturbed tubulin polymerization, arrested cells in the G_2/M phase, induced apoptosis, and displayed potent antiproliferative activities against prostate and melanoma cell lines *in vitro* and *in vivo*. Consistent with these biological effects, the *in vivo* antiproliferative activity of SMART-H and SMART-F were greater than SMART-OH.

Currently, there are many potential microtubule stabilizers or destabilizers in various stages of development (14). Some antimitotic compounds, such as the vinca alkaloids and taxanes, are already in clinical use. However, the vinca alkaloids and taxanes are substrates of P-gp, which pumps drugs out of cancer cells and is thought to limits their effectiveness. Compared to other drug classes, antitubulin agents have somewhat different resistance mechanisms. For example, over-expression of P-glycoprotein, changes in microtubule dynamics (15) and mutations in β-tubulin are known to limit sensitivity to the taxanes (16). Two mechanisms of drug resistance have been examined with the SMART compounds in this study: (a) the presence of drug efflux pumps and (b) development of drug resistance by tumor *in vivo*. We tested SMART compounds against a cell line that over-expresses P-gp. Notably, the SMART compounds demonstrated equi-potent anti-proliferative effects against OVCAR-8 (parent) and NCI/ADR-RES (MDR-positive) cell line, suggesting that SMART compounds are not P-gp substrates and that they function in a P-gp-independent manner. This feature differs from that of paclitaxel, vinblastine, and colchicine in NCI/ADR-RES cells. We also examined the cytotoxicity of SMART-H in PC-3 tumor cells (*in vivo*) excised from mice, which were treated with 15 mg/kg SMART-H for 21 days. SMART-H equi-potently inhibited the growth of cells derived from the primary tumor cell culture and ATCC PC-3 cell line, indicating that prolonged treatment with SMART-H did not develop drug resistance in PC-3 tumors over 21 days.

Many drug candidates encounter problems during development associated with chemical instability, high metabolic clearance, and peripheral neurotoxicity (17–19). We performed PK studies with the SMART compounds in mice, and found that the SMART compounds exhibited high clearance. Based on metabolic stability studies using liver microsomes *in vitro*, we predicted that the high clearance observed in mice may be due to rapid hepatic metabolism (C. M. Li et al, manuscript submitted for publication). However, the SMART compounds exhibited species differences in metabolism, and were more stable in liver microsomes obtained from rats, dogs and human. We also performed PK studies in rats. Total plasma clearances of SMART-H and -F in rats were 6 and 11 ml/min/kg, respectively, indicative of a low hepatic extraction rate (rat hepatic blood rate is 55 ml/min/kg (14)). These PK data demonstrate that *in vitro* metabolic stability studies provided a reliable prediction for *in vivo* clearance in animals. It is hoped that xenograft studies in mice may underestimate the antitumor efficacy achievable in humans due to inter-species differences in metabolism. We developed a suitable formulation to increase drug exposure after intraperitoneal injection. We compared the AUC (drug exposure) using two different formulations and intraperitoneal injection prior to the initiation of tumor xenograft studies. SMART-H (15 mg/kg) in Captex200/Tween80 (1/4) exhibited 4-fold higher AUC compared to the PEG300/DMSO (1/4) formulation, indicating that the Captex200/Tween80 (1/4) formulation facilitated a greater exposure to SMART-H (data not shown). Based on PK data (high clearance and short half-life) from mice, we employed a high frequency dosing regimen. The promising *in vivo* antitumor activity of SMART-H and SMART-F in a species that rapidly eliminates these drugs, coupled with their improved stability in human liver

microsomes, further supports the view that these SMART compounds may possess better anticancer activity in human patients than in mice with prostate cancer or melanoma xenografts.

One of the major adverse events associated with antitubulin agents is peripheral neurotoxicity. The rotarod assay has been used to examine *in vivo* neurotoxicity (20,21). In this report, the rotarod assay was conducted to test peripheral neurotoxicity of SMART-H in ICR mice. Mice treated with SMART-H did not show significant impairment in motor coordination compared to that of mice in the vehicle group. The positive control, vinblastine-treated group, demonstrated a lesser ability to stay on the rotating rod, indicative of neurotoxicity. We also extended the experiment for 4 weeks after drug treatment was stopped, and found that the ability of the vinblastine-treated group to stay on the rotating rod failed to return to baseline or to values of the vehicle-treated group, indicating that neurotoxicity was only be partially reversible with time. The post-observation also ruled out delayed neurotoxicity in SMART treatment groups. These data provide compelling evidence that we have developed a novel family of SMART compounds with lesser neurotoxicity.

Prostate cancer PC-3 and melanoma A375 cells were chosen to examine the activity of SMART compounds *in vivo* because SMART compounds exhibited greater potency in these cancer cell lines *in vitro*. A375 xenografts exhibited higher tumor growth rate than PC-3 xenografts. This corresponded well with their *in vitro* growth rate. In this report, SMART-H and SMART-F both showed significant efficacy on both low and high growth rate xenograft models *in vivo*. Compared to the control groups, SMART-H and –F inhibited tumor growth significantly at doses between 5 and 20 mg/kg. We obtained %T/C indices of 4 to 30% with SMART-H and -F treatments in both xenograft models. Under conditions of initial efficacy testing, it would appear that SMART-H at 15 mg/kg, ip, qDx21 is the most active treatment regimen (a T/C = 4% is recorded in Table 3). Moreover, in Figure 4A, a plot of mean tumor masses shows a reduction in tumor masses on day 3 with at least partially regressed tumors and/or a continuation of blunted growth over the remaining duration of treatment. Interesting, we found that tumor sizes were lower than their initial sizes (150 mm^3) in 4 of 7 mice after 21 days treatment, suggesting that this treatment elicited partial regression in these animals. Animal body weight measurements in the PC-3 tumor model showed that 1/8 mice treated with SMART-H at 15 mg/kg and 2/7 mice treated with SMART-F lost more than 15% body weight within 21 days of treatment. However, no appreciable animal body weight losses data were identified for the A 375 model treated longer (for 34 days) with SMART-H at 20 mg/kg or SMART-F at 15 mg/kg. It was thought that 15~20 mg/kg of SMART-H and –F are close to the boundary of toxicity, and hence, we obtained 15% body weight loss in one animal study, not in the other. To confirm index of drug toxicity, we will need more treatment groups, such as 10 and 25 mg/kg treatments in further studies. Though SMART-OH, was tested at a dose higher than that of SMART-H and SMART-F, and demonstrated more favorable pharmacokinetic properties, it exhibited 10-fold less potency than SMART-H at higher dosage in the PC-3 xenograft model (Fig. 4A). Thus, the lower tubulin inhibitory potency of SMART-OH was not sufficiently compensated by its lower clearance and greater exposure. These data further suggest that SMART-OH, if a metabolite of SMART-H, would contribute little, if any, to the *in vivo* anticancer activity of SMART-H.

In summary, we have demonstrated that SMART compounds are potent antitubulin compounds that overcome P-gp-mediated drug resistance *in vitro* and which, in fact, are highly active anticancer agents both *in vitro* and *in vivo*. In contrast to three clinical antitubulin agents, SMART compounds are highly active in an Adriamycin-resistant cancer cell line. The efficacy studies revealed that SMART compounds have activities in PC-3 and A375 cancer xenografts. Importantly, SMART-H did not show neurotoxicity *in vivo* and tumor cells treated *in vivo* did not develop drug resistance. The *in vitro* and *in vivo*

anticancer effect of the SMART compounds and the lesser neurotoxicity observed in this study serve as a pre-clinical basis to suggest that these novel compounds may have therapeutic potential for cancer therapy in the clinic.

References

1. Hadfield JA, Ducki S, Hirst N, McGown AT. Tubulin and microtubules as targets for anticancer drugs. Prog Cell Cycle Res 2003;5:309–325. [PubMed: 14593726]
2. Honore S, Pasquier E, Braguer D. Understanding microtubule dynamics for improved cancer therapy. Cell Mol Life Sci 2005;62:3039–3056. [PubMed: 16314924]
3. Jordan A, Hadfield JA, Lawrence NJ, McGown AT. Tubulin as a target for anticancer drugs: agents which interact with the mitotic spindle. Med Res Rev 1998;18:259–296. [PubMed: 9664292]
4. Jordan MA, Kamath K. How do microtubule-targeted drugs work? An overview. Curr Cancer Drug Targets 2007;7:730–742. [PubMed: 18220533]
5. Perez EA. Microtubule inhibitors: Differentiating tubulin-inhibiting agents based on mechanisms of action, clinical activity, and resistance. Mol Cancer Ther 2009;8:2086–2095. [PubMed: 19671735]
6. Heinz DW, Schubert WD, Hofle G. Much anticipated--the bioactive conformation of epothilone and its binding to tubulin. Angew Chem Int Ed Engl 2005;44:1298–1301. [PubMed: 15714588]
7. Lee FY, Borzilleri R, Fairchild CR, Kamath A, Smykla R, Kramer R, Vite G. Preclinical discovery of ixabepilone, a highly active antineoplastic agent. Cancer Chemother Pharmacol 2008;63:157–166. [PubMed: 18347795]
8. Polgar O, Bates SE. ABC transporters in the balance: is there a role in multidrug resistance? Biochem Soc Trans 2005;33:241–245. [PubMed: 15667317]
9. Michels J, Ellard SL, Le L, Kollmannsberger C, Murray N, Tomlinson Guns ES, Carr R, Chi KN. A phase IB study of ABT-751 in combination with docetaxel in patients with advanced castration-resistant prostate cancer. Ann Oncol 2010;21:305–311. [PubMed: 19633045]
10. Fox E, Maris JM, Widemann BC, Goodspeed W, Goodwin A, Kromplewski M, Fouts ME, Medina D, Cohn SL, Krivoshik A, Hagey AE, Adamson PC, Balis FM. A phase I study of ABT-751, an orally bioavailable tubulin inhibitor, administered daily for 21 days every 28 days in pediatric patients with solid tumors. Clin Cancer Res 2008;14:1111–1115. [PubMed: 18281544]
11. Lu Y, Li CM, Wang Z, Ross CR II, Chen J, Dalton JT, Li W, Miller DD. Discovery of 4-substituted methoxybenzoyl-aryl-thiazole as novel anticancer agents: synthesis, biological evaluation, and structure-activity relationships. J Med Chem 2009;52:1701–1711. [PubMed: 19243174]
12. Alley, MC.; Hollingshead, MG.; Dykes, DJ.; Waud, WR. Human tumor xenograft models in NCI drug development. In: Teicher, BA.; Andrews, PA., editors. Anticancer drug development guide. New Jersey: Humana Press; 2004. p. 125-152.
13. Davies B, Morris T. Physiological parameters in laboratory animals and humans. Pharm Res 1993;10:1093–1095. [PubMed: 8378254]
14. Jordan MA, Wilson L. Microtubules as a target for anticancer drugs. Nat Rev Cancer 2004;4:253–265. [PubMed: 15057285]
15. Goncalves A, Braguer D, Kamath K, Martello L, Briand C, Horwitz S, Wilson L, Jordan MA. Resistance to Taxol in lung cancer cells associated with increased microtubule dynamics. Proc Natl Acad Sci U S A 2001;98:11737–11742. [PubMed: 11562465]
16. Monzo M, Rosell R, Sanchez JJ, Lee JS, O'Brate A, Gonzalez-Larriba JL, Alberola V, Lorenzo JC, Nunez L, Ro JY, Martin C. Paclitaxel resistance in non-small-cell lung cancer associated with beta-tubulin gene mutations. J Clin Oncol 1999;17:1786–1793. [PubMed: 10561216]
17. Lin JH, Lu AY. Role of pharmacokinetics and metabolism in drug discovery and development. Pharmacol Rev 1997;49:403–449. [PubMed: 9443165]
18. Fukuda DS, Mabe JA, Brannon DR. Production of substituted L-tryptophans by fermentation. Appl Microbiol 1971;21:841–843. [PubMed: 5574318]
19. Windebank AJ. Chemotherapeutic neuropathy. Curr Opin Neurol 1999;12:565–571. [PubMed: 10590893]

20. Nakai R, Iida S, Takahashi T, Tsujita T, Okamoto S, Takada C, Akasaka K, Ichikawa S, Ishida H, Kusaka H, Akinaga S, Murakata C, Honda S, Nitta M, Saya H, Yamashita Y. K858, a novel inhibitor of mitotic kinesin Eg5 and antitumor agent, induces cell death in cancer cells. Cancer Res 2009;69:3901–3909. [PubMed: 19351824]

21. Bacher G, Nickel B, Emig P, Vanhoefer U, Seeber S, Shandra A, Klenner T, Beckers T. D-24851, a novel synthetic microtubule inhibitor, exerts curative antitumoral activity in vivo, shows efficacy toward multidrug-resistant tumor cells, and lacks neurotoxicity. Cancer Res 2001;61:392–399. [PubMed: 11196193]

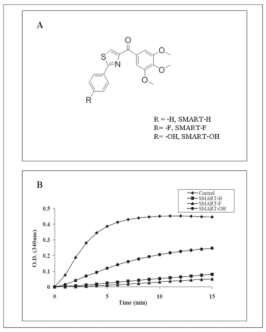

Figure 1.

SMART compounds inhibit tubulin polymerization via binding to the colchicine binding site on tubulin. (*A*) Structures of SMART-H, -F, and –OH. (*B*) Effect of SMART compounds on tubulin polymerization. Tubulin (0.4 mg) was exposed to SMART compounds (10 μM). Absorbance at 340 nm was monitored every min for 15 min.

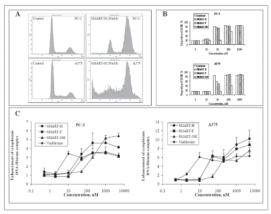

Figure 2.

SMART compounds arrested cells into G_2/M phase and induced apoptosis. (*A*) Representative graphs of cell cycle analysis after compounds treatment for 24 h on PC-3 and A375 cells. (*B*) The changes in G_2/M proportion induced by SMART-H, -F, and –OH in PC-3 and A375 cells after 24h treatment. (*C*) Ability of SMART-H, -F, and –OH to enhance cytoplasmic DNA-Histone complex formation in 24h (n = 3); bars, SD. Colchicine and vinblastine were used as positive controls.

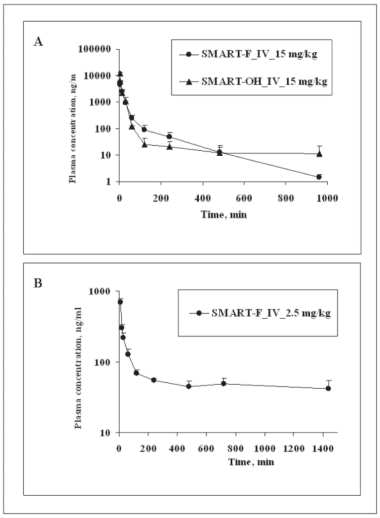

Figure 3.

Pharmacokinetic studies of SMART-F, and -OH in mice and rats. (*A*) Concentration-time curve of SMARTs in ICR mice (n = 3); bars, SD. SMARTs were administrated 15mg/kg i.v. by tail vein injection. (*B*) Concentration-time curve of SMART-F in SD rats (n = 4); bars, SD. SD rats were dosed 2.5 mg/kg i.v. with the formulation DMSO/PEG300 (1/4). The pharmacokinetic data for SMART-H are shown for comparison, and were previously presented in Li et al. (Drug Metabolism and Disposition 2010).

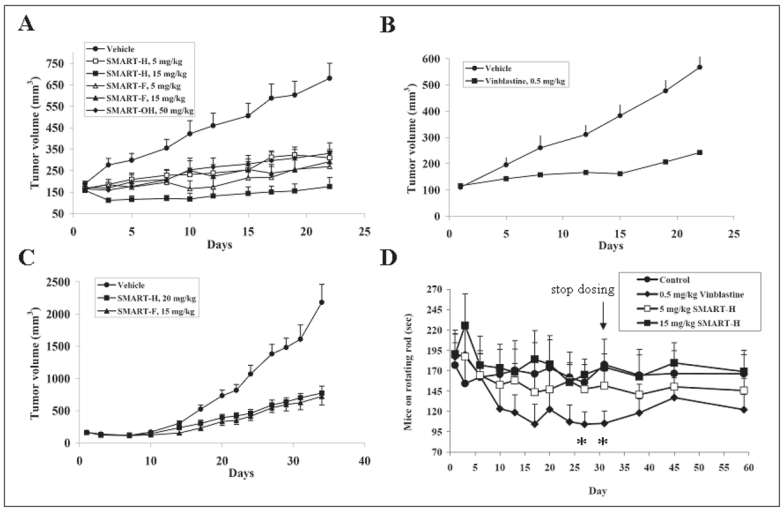

Figure 4.

In vivo anti-cancer efficacy and neurotoxicity of SMART compounds. (*A*) SMARTs efficacy for PC-3 prostate tumor xenografted on nude mice (n = 6–8). (*B*) Vinblastine efficacy for PC-3 prostate tumor xenografted on nude mice (n = 8). This served as the positive control. (*C*) *In vivo* efficacy of SMART-H and SMART-F in nude mice bearing A375 melanoma xenografts (n = 10). Nude mice were inoculated 2.5×10^6 PC-3 or A375 cells and dosed i.p. daily (SMART compounds) and q2d (vinblastine) after tumor formation (150–200 mm^3). Each point represents mean tumor volume for animals in each group. (*D*) *In vivo* neurotoxicity (rotarod test) of SMART-H in ICR mice (n = 7 or 8). SMART-H (5 and 15 mg/kg), vinblastine (0.5 mg/kg) and vehivle were given i.p. daily, and vinblastine was used as the positive control. The dosing was stopped on day 31. *, $p < 0.05$. Bars, SE

Table 1

In vitro efficacy of SMART compounds on prostate, melanoma and drug resistant cell lines (n = 3, mean ± SE). Paciltaxel, vinblastine, and colchicine were used as positive controls.

		IC_{50} ± SEM (nM)					
Cell line	**Cell type**	**SMART-H**	**SMART-F**	**SMART-OH**	**Paclitaxel**	**Vinblastine**	**Colchicine**
LNCaP	Prostate	28 ± 4[a]	6 ± 1[a]	103 ± 9	1.7 ± 0.2	1.1 ± 0.1	16 ± 4
PC-3	Prostate	21 ± 1[a]	13 ± 1[a]	87 ± 5	4.8 ± 0.3	2.1 ± 0.2	11 ± 1
Du-145	Prostate	71 ± 4[a]	12 ± 1[a]	116 ± 14	5.1 ± 0.1	1.8 ± 1.1	10 ± 2
PPC-1	Prostate	43 ± 5[a]	8 ± 1[a]	76 ±2	2.3 ± 0.8	1.1 ± 0.4	20 ± 1
B16-F1	Melanoma	55 ± 5[a]	43 ± 21[a]	113 ± 6	17 ± 2	4.7 ± 0.7	29 ± 5
A375	Melanoma	28 ± 5[a]	33 ± 14[a]	93 ± 11	12 ± 3	1.1 ± 0.2	20 ± 3
OVCAR-8	Ovarian	35 ± 2	34 ± 3	110 ± 8	4.7 ± 0.1	3.9 ± 0.1	17 ± 1
NCI/ADR-RES	Ovarian	13 ± 1	12 ± 1	45 ± 5	6263 ± 634	582 ± 57	1113 ± 79
Resistance Factor		0.4	0.4	0.4	1333	149	65

[a]Previously reported in reference (11).

Table 2

Pharmacokinetic parameters of SMART compounds. SMARTs were administrated 15 mg/kg and 2.5 mg/kg i.v. in mice and rats, respectively.

***In vivo*, pharmacokinetic parameters of SMART compounds**					
Species	**Parameter**	**Unit**	**SMART-H**	**SMART-F**	**SMART-OH**
Mice	AUC	hr * μg/mL	1.9[a]	2.2	2.6
	$t_{1/2}$	min	140[a]	141	740
	V_{ss}	L/kg	4.9[a]	6.6	16.5
	CL	mL/min/kg	130[a]	112	90
Rats	AUC	hr * μg/mL	5.8[a]	1.6	NA
	$t_{1/2}$	min	1431[a]	2410	NA
	V_{ss}	L/kg	7.6[a]	34	NA
	CL	mL/min/kg	6[a]	11	NA

[a] C. M. Li et al, in press.

Table 3

In vivo treatment of human tumor xenografts. %T/C values < 40% are considered to be active by criteria of the National Cancer Institute criteria (12).

Compound	Dosage (mg/kg)	Xenograft model	% T/C
Vehicle	NA	Prostate	100
Vinblastine	0.5	Prostate	29
SMART-H	5	Prostate	29
SMART-H	15	Prostate	4
SMART-F	5	Prostate	21
SMART-F	15	Prostate	24
SMART-OH	50	Prostate	34
Vehicle	NA	Melanoma	100
SMART-H	20	Melanoma	30
SMART-F	15	Melanoma	28